



Hyperspectral remote sensing of cyanobacteria in turbid productive water using optically active pigments, chlorophyll *a* and phycocyanin

Kaylan Randolph^{a,d,*}, Jeff Wilson^a, Lenore Tedesco^{b,d}, Lin Li^b, D. Lani Pascual^d, Emmanuel Soyeux^c

^a Department of Geography, Indiana University–Purdue University, Indianapolis, United States

^b Department of Earth Sciences, Indiana University–Purdue University, Indianapolis, United States

^c Veolia Environnement, France

^d Center for Earth and Environmental Science, Indiana University–Purdue University, Indianapolis, United States

ARTICLE INFO

Article history:

Received 26 March 2007

Received in revised form 19 May 2008

Accepted 5 June 2008

Keywords:

Hyperspectral
Remote sensing
Cyanobacteria
Phycocyanin
Chlorophyll *a*
Blue-green algae

ABSTRACT

Nuisance blue-green algal blooms contribute to aesthetic degradation of water resources by means of accelerated eutrophication, taste and odor problems, and the production of toxins that can have serious adverse human health effects. Current field-based methods for detecting blooms are costly and time consuming, delaying management decisions. Methods have been developed for estimating phycocyanin concentration, the accessory pigment unique to freshwater blue-green algae, in productive inland water. By employing the known optical properties of phycocyanin, researchers have evaluated the utility of field-collected spectral response patterns for determining concentrations of phycocyanin pigments and ultimately blue-green algal abundance. The purpose of this research was to evaluate field spectroscopy as a rapid cyanobacteria bloom assessment method. *In-situ* field reflectance spectra were collected at 54 sampling sites on two turbid reservoirs on September 6th and 7th in Indianapolis, Indiana using ASD Fieldspec (UV/VNIR) spectroradiometers. Surface water samples were analyzed for *in-vitro* pigment concentrations and other physical and chemical water quality parameters. Semi-empirical algorithms by Simis et al. [Simis, S., Peters, S., Gons, H. (2005). Remote sensing of the cyanobacterial pigment phycocyanin in turbid inland water. *American Society of Limnology and Oceanography* 50(11): 237–245] were applied to the field spectra to predict chlorophyll *a* and phycocyanin absorption at 665 nm and 620 nm, respectively. For estimation of phycocyanin concentration, a specific absorption coefficient of $0.0070 \text{ m}^2 \text{ mg PC}^{-1}$ for phycocyanin at 620 nm, $a_{\text{PC}}^*(620)$, was employed, yielding an r^2 value of 0.85 ($n=48$, $p<0.0001$), mean relative residual value of 0.51 ($\sigma=1.41$) and root mean square error (RMSE) of 19.54 ppb. Results suggest this algorithm could be a robust model for estimating phycocyanin. Error is highest in water with phycocyanin concentrations of less than 10 ppb and where phycocyanin abundance is low relative to chlorophyll *a*. A strong correlation between measured phycocyanin concentrations and biovolume measurements of cyanobacteria was also observed ($r=0.89$), while a weaker relationship ($r=0.66$) resulted between chlorophyll *a* concentration and cyanobacterial biovolume.

© 2008 Elsevier Inc. All rights reserved.

1. Introduction

Nuisance algal blooms cause aesthetic degradation to lakes and reservoirs resulting in surface scum, unpleasant taste and odor in drinking water (from the production of metabolites such as methyl isoborneol and geosmin), and possible adverse effects to human health from blue-green algal toxins. Though cyanobacterial genera observed in Midwestern reservoirs, including *Anabaena*, *Oscillatoria*,

Microcystis, and *Cylindrospermopsis*, have been documented as toxin producers, the conditions in which they produce toxins are highly variable. Predicting the locations and timing of blue-green blooms using traditional sampling techniques is difficult, if not impossible (Backer, 2002; Pitois et al., 2000). Because the acute effects of intoxication are severe, stringent monitoring programs of cyanobacteria blooms in drinking water and recreational reservoirs are necessary. Current methods consist of field sample collection, laboratory analysis, and identification and enumeration of phytoplankton, which can take days to weeks. These methods are neither timely nor cost efficient for drinking water managers since blooms can be as ephemeral as a few days. However, because phytoplankton pigments are optically active, their properties can be measured using spectroscopy.

* Corresponding author. Department of Geography, Indiana University–Purdue University, Indianapolis, United States.

E-mail address: kaylan.randolph@uconn.edu (K. Randolph).

Many algorithms have been proposed for estimating chlorophyll *a* as a proxy for productivity in turbid water (e.g., Gitelson et al., 1986; Mittenzwey et al., 1992). Fewer methods have been developed for predicting phycocyanin, the accessory pigment unique to freshwater blue-green algae, in productive inland water. Since blue-green algae have a unique accessory pigment, by employing the known properties of phycocyanin, researchers have evaluated the utility of field-collected spectral response patterns for determining concentrations of phycocyanin pigments and ultimately blue-green algal abundance (e.g., Dekker, 1993; Dekker et al., 1991; Schalles and Yacobi, 2000; Simis et al., 2005). These researchers have developed models based on variability of spectral response gathered by medium to high resolution spectroradiometers (spectral range approximately 300 to 1100 nm) for sites with differing algal density. Models are often applied using an empirical approach where relationships between spectral reflectance and laboratory-measured constituent concentrations are developed using statistical methods. Algorithms employing the empirical approach, however, have proven to be less robust and transferable to other lakes or sensors because they require coefficients obtained in regression analysis for obtaining pigment concentration. Semi-empirical models used to derive the absorption coefficient for phycocyanin by applying previously discovered empirical relationships and the inherent optical properties, the scattering and absorption properties of the water and its constituents, have potential to be robust (Preisendorfer, 1976; Dekker et al., 1991; Simis et al., 2005).

The purpose of this research is to extend and validate a semi-empirical remote sensing method proposed by Simis et al. (2005) for mapping the relative concentration of cyanobacteria in turbid, inland reservoirs. Developed in inland productive (case II) water where chemistry is complex including high concentrations of phytoplankton pigments, inorganic suspended material, non-algal suspended matter, and colored dissolved organic matter, the Simis et al. (2005) algorithm has potential for application to other turbid eutrophic reservoirs. The algorithm was evaluated for accuracy in estimating analytically measured phycocyanin concentrations from field spectral response measurements collected in two Indianapolis, Indiana reservoirs.

1.1. Background

Recent research in remote sensing of water quality suggests a movement from the empirical to a semi-analytical or bio-optical modeling technique, where radiative transfer (ERT) is used to deconvolve water-leaving radiance to obtain the inherent optical properties (IOPs) of the water body (the absorption and scattering characteristics) and subsequently, the biogeochemical parameters of interest (i.e., GSM of Maritorena and Siegel, 2005, QAA of Lee et al., 2005). Biogeochemical parameters are related to remotely sensed radiance using their specific absorption coefficients, absorption per unit path length per unit mass concentration (Morel and Gordon, 1980; Dekker, 1993). The analytical approach reduces the use of the statistically derived coefficients used in empirical modeling, relating the remotely sensed radiance to water quality parameters, and instead employs what is known about the optical properties of the water and light field.

Bio-optical modeling for turbid inland water has proven difficult because the optical properties of the water body are not solely dependent on phytoplankton and its byproducts, but also on colored dissolved organic matter (CDOM), inorganic suspended matter (ISM), and non-algal organic matter. The spectral characteristics of CDOM and ISM are highly variable due to differences in particle shape, size, and composition (Morel, 2001). Further, researchers exploring the optical characteristics of cyanobacteria have discovered that the specific absorption coefficient is highly variable both inter- and intra-species, dependent on the cell

physiology, morphology and the photoadaptive response of cells to change under different environmental conditions (Kirk, 1994; Morel, 2001; Simis et al., 2005).

The Simis et al. (2005) semi-empirical model is based on the relationship between subsurface irradiance reflectance ($R(O^-, \lambda)$) and the absorption and backscatter coefficients for the optically active constituents in the water column (Gordon et al., 1975):

$$R(O^-, \lambda) = f \frac{b_b(\lambda)}{a(\lambda) + b_b(\lambda)} \quad (1)$$

Where:

$R(O^-, \lambda)$	subsurface irradiance reflectance at a specified depth and wavelength
f	experimental scaling factor dependent on the light field (sun angle) and volume scattering function (VSF) (Morel & Gentili, 1991)
$b_b(\lambda)$	total backscatter coefficient
$a(\lambda)$	total absorption coefficient

To determine the phycocyanin absorption coefficient, the algorithm requires estimation of chlorophyll *a*, ultimately used as a correction for its effects on the spectral region of interest for estimating phycocyanin concentration. Two empirical models, which utilize the relationship between the wavelength location of maximal scattering by algal cells (minimal absorption by pigments) and the wavelength location of maximal pigment absorption efficiency (Morel and Prieur, 1977; Gitelson et al., 1999), were employed for estimating chlorophyll *a* (Eq. (2)) and phycocyanin (Eq. (3)):

$$\text{Chlorophyll } a : \frac{R(709)}{R(665)} \quad (2)$$

$$\text{Phycocyanin} : \frac{R(709)}{R(620)}. \quad (3)$$

The proposed ratios are based on the high sensitivity of the features found at 665 and 620 nm to change in chlorophyll *a* and phycocyanin concentration. Variability in these features along a continuum of pigment density could therefore be used in an algorithm for predicting chlorophyll *a* and phycocyanin prevalence from reflectance spectra (Gitelson et al., 1986; Mittenzwey and Gitelson, 1988; Mittenzwey et al., 1992; Gitelson et al., 1993; Dekker, 1993; Jupp et al., 1994). It is assumed that absorption at 665 nm is a function of both chlorophyll *a* (Chl) and pure water, thus $a(665) = a_{chl}(665) + a_w(665)$. Similarly, absorption at 620 nm is assumed to be the sum of absorption by pure water, phycocyanin (PC), chlorophyll *a* where

$$a(620) = a_{pc}(620) + a_{chl}(620) + a_w(620).$$

The absorption coefficients for pure water at the wavelengths of interest, $a_w(665)$ and $a_w(620)$ (Pope and Fry, 1997; Buiteveld et al., 1994), and the total backscattering coefficient, b_b , retrieved from the reflectance signal at 778 nm, as suggested by Gons (1999) are included to differentiate absorption by pigments. Retrieval of b_b requires the use of a constant (α) to account for refraction at the water's surface. The following algorithms were introduced for derivation of the chlorophyll *a* and phycocyanin absorption coefficients at 665 and 620 nm, respectively:

$$a_{chl}(665) = \left(\left\{ \frac{R(709)}{R(665)} [a_w(709) + b_b] \right\} - b_b - a_w(665) \right) \gamma^{-1} \quad (4)$$

$$a_{PC}(620) = \left(\left(\frac{R(709)}{R(620)} [a_w(709) + b_b] \right) - b_b - a_w(620) \right) \delta^{-1} - [(\varepsilon) a_{chl}(665)] \quad (5)$$

Where:

- $a_{chl}(665)$ = absorption of chlorophyll *a* at 665 nm
 $a_{PC}(620)$ = absorption of phycocyanin at 620 nm
 $R(\lambda)$ = reflectance value at a specified wavelength
 $a_w(\lambda)$ = pure water absorption coefficients at specified locations (Buiteveld et al., 1994)
 $a_w(709) = 0.727 \text{ m}^{-1}$
 $a_w(665) = 0.401 \text{ m}^{-1}$
 $a_w(620) = 0.281 \text{ m}^{-1}$
 $a_w(778) = 2.71 \text{ m}^{-1}$
 $b_b = [a_w(778)\alpha R(778)][\gamma' - \alpha R(778)]^{-1}$ (Gordon, et al., 1988; Gons, 1999; Astoreca et al., 2006)
 $\alpha = 0.60$, accounts for refraction at the water surface
 $\gamma' = 0.082$, experimental factor based on average cosine of downward irradiance (Gordon, et al., 1988; Astoreca et al., 2006)
 $\gamma = 0.68$, a constant derived from the linear least-squares fit of measured $a(665)$ (using filter-pad technique) to estimated chlorophyll *a* absorption, derived from Lake Loosdrecht data (Simis et al., 2005)
 $\delta = 0.84$, correction factor derived from the linear least-squares fit of measured $a(620)$ (using filter-pad technique) to estimated phycocyanin absorption, derived from Lake Loosdrecht data (Simis et al., 2005)
 $\varepsilon = 0.24$; proportion of $a(620)$ attributed to chlorophyll *a*, derived from Lake Loosdrecht data (Simis et al., 2005)

Assuming a linear relationship between the absorption and scattering properties of a water body and the concentration of its constituents, the ratio of the absorption coefficient for the optically active constituent of interest to the specific absorption coefficient, $a_i^*(\lambda)$ absorption per unit path length and mass concentration, yields an estimate of pigment concentration ($\text{m}^2 \text{ mg pigment}^{-1}$; Gons, 1999; Simis et al., 2005):

$$[\text{Pigment}]_i = \frac{a_i(\lambda)}{a_i^*(\lambda)} \quad (6)$$

Concentration of chlorophyll *a* and phycocyanin can then be determined from:

$$[\text{Chl}] = \frac{a_{chl}(665)}{a_{chl}^*(665)} \quad (7)$$

$$[\text{PC}] = \frac{a_{PC}(620)}{a_{PC}^*(620)} \quad (8)$$

Where:

- $a_{chl}(665)$ absorption by chlorophyll *a* at 665 nm, estimated using Eq. (4)
 $a_{chl}^*(665)$ $0.0153 \text{ m}^2 \text{ mg Chl}^{-1}$, average pigment specific absorption value for chlorophyll *a* at 665 nm for various lakes and reservoirs in Spain and The Netherlands (taken from Simis et al., 2005 and 2006)
 $a_{PC}^*(620)$ Absorption by phycocyanin at 620 nm, estimated using Eq. (5)
 $a_{PC}^*(620)$ $0.0070 \text{ m}^2 \text{ mg PC}^{-1}$, average pigment specific absorption value for phycocyanin at 620 nm for various lakes and

reservoirs in Spain and The Netherlands (taken from Simis et al., 2006)

2. Study site description

Geist (W 85°56'29.5749", N 39°55'32.1001") and Morse (W 86°2'17.2291", N 40°6'16.84512") Reservoirs are small (approximately 7 km²), shallow systems (mean depth of 5 m). Both reservoirs are an integral part of the water supply network for the City of Indianapolis, Indiana. Increases in residential and agricultural development have brought a subsequent increased loading of nutrients to the reservoirs (classified as meso- to eutrophic), ultimately enhancing blue-green bloom time and magnitude (Table 1; Tedesco et al., 2003).

3. Methodology

3.1. Field methodology

On September 6 and 7, 2005, above surface radiometry and ground truth data were collected at 55 sampling sites on Morse (28 sites) and Geist (27 sites) Reservoirs (Fig. 1). Sampling sites were selected to span the entire surface of each reservoir (Table 1). Sampling station quantity was determined as that which provided sufficient representation of the whole system including both deep and shallow areas, coves and main basins.

Downwelling radiance and upwelling total radiance measurements were collected at each of the sampling sites using an ASD FieldSpec UV–VNIR (Analytical Devices, Inc., Boulder, CO) spectroradiometer. The ASD FieldSpec radiometer records a continuous spectrum in 708 bands within a spectral range from 348 to 1074 nm. Sky conditions were completely clear during the entire field sampling campaign. Total upwelling radiance, L_t ($\text{W m}^{-2} \text{ sr}^{-1}$) was measured using an optical fiber attached to an extendable pole (to eliminate the influence of the vessel) pointed in a nadir viewing angle ($\phi = 90^\circ$) set at a height of approximately 0.5 m above the water surface. Radiometric measurements were collected before solar noon, when the sun zenith angle was less than 60° . The instantaneous-field-of-view (IFOV) of the bare optical fiber was 0.17 rad, producing a diameter of 0.04 m on the water surface. L_t measured in this study was corrected for the influence of sky radiance reflected by the surface (L_{sky}) by subtracting $R_{rs}(900)$ from the R_{rs} spectra, assuming any signal received at this wavelength location is attributed to L_{sky} .

Table 1

Description of Geist and Morse Reservoirs and their corresponding watersheds, Fall Creek and Cicero Creek

Reservoir	Geist	Morse	Units
Surface area	7.5	6.0	km ²
Reservoir volume	23.8	28.0	million m ³
Maximum depth	14.7	12.9	m
Mean depth	3.2	4.7	m
Residence time	55	70	days
Trophic status	Mesotrophic ^a	Eutrophic ^b	
Mean total P	100 ^b	94 ^b	μg P/L
Mean total N	2.0 ^b	4.1 ^b	mg N/L
% Agriculture in watershed	58.3% ^c	76.9% ^c	
Trunk stream (median flow)	Fall Creek (2.6) (91.8)	Cicero Creek (1.0) (35.3)	m ³ /s cfs
Dominant phytoplankton	<i>Aulacoseira</i> , <i>Scenedesmus</i> / <i>Ankistrodesmus</i> , <i>Aphanizomenon/Anabaena</i>	<i>Aulacoseira</i> , <i>Scenedesmus</i> / <i>Ankistrodesmus</i> , <i>Aphanizomenon/Anabaena</i>	

^a IDEM (2002, 2004, 2006).

^b Various CIWRP studies, including this study, from 2003–2005.

^c Eagle Creek Land cover assessments (Tedesco et al., 2005) and 2000 land use/land cover assessments for Fall Creek and Cicero Creek Watersheds (Tedesco et al., 2003).

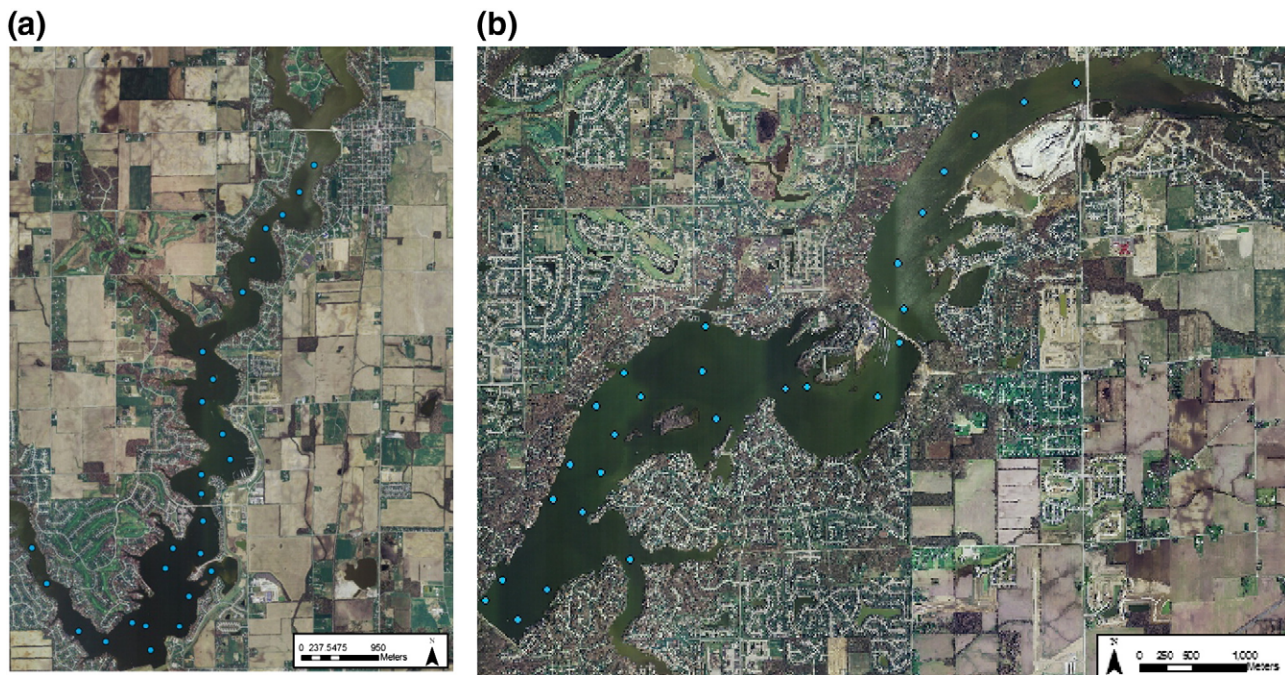


Fig. 1. a and b: Sampling sites on (a) Morse (W 86°2'17.2291", N 40°6'16.84512") and (b) Geist (W 85°56'29.5749", N 39°55'32.1001") Reservoirs (March 2005, IGIC).

Placid water, clear sky conditions, where wind speed is 0 m s^{-1} prevailed during collection of this dataset. To eliminate spectra potentially affected by sun glint and to optimize the signal-to-noise ratio, inconsistent radiance measurements were removed and the final measurement at each site was the average over 15 readings. Downwelling radiance measurements, L_d ($\text{W m}^{-2} \text{ sr}^{-1}$) were collected at each sample site using a 99% spectralon panel as an optical standard for calibrating upwelling radiance. A dark reference was collected with each measurement of L_d .

Secchi depth (cm) was collected at each site to estimate water transparency. The following physical parameters were measured at the 55 sampling sites on Geist and Morse Reservoirs using YSI multi-parameter probes (model 600XLM-SV) positioned 25 cm below the water surface: temperature ($^{\circ}\text{C}$), specific conductance (mS), total dissolved solids (g/L), salinity (ppt), DO (% and mg/L), and pH.

3.2. Water sample analysis

Surface water grab samples were collected at each station and analyzed for chlorophyll *a*, phycocyanin, and other water quality constituents including total suspended solids (TSS), turbidity, total Kjeldahl nitrogen (TKN), total phosphorus, ortho-phosphorus, and loss-on-ignition carbon (LOI) at IUPUI laboratories. Other secondary physical and chemical analyses were performed by Veolia Water Indianapolis, LLC using the Environmental Protection Agency and American Public Health Association standards.

3.3. Pigment analysis

Samples analyzed for chlorophyll *a* and phycocyanin were collected in 1 L amber HDPE bottles and filtered and frozen within 4 h to preserve pigments. All steps in the pigment extraction process were performed under subdued light conditions.

3.3.1. Chlorophyll *a*

Samples were filtered through 47 mm, $0.45 \mu\text{m}$ pore size acetate filters using a filtration manifold. For each sample, a replicate was also filtered. Filters were frozen for 20–30 days until analysis. Filters were

dissolved in 90% buffered acetone¹ and allowed to extract in the freezer (-3°C) for at least 24 h and no longer than 48 h. Extracted chlorophyll *a* was analyzed using the Environmental Protection Agency method 445.0 (1983). Pheophytin corrected chlorophyll *a* was measured fluorometrically using a TD-700 Fluorometer (Turner Designs, Inc.) equipped with a Daylight White Lamp and Chlorophyll Optical Kit (340–500 nm excitation filter and emission filter 665 nm) and calibrated with chlorophyll *a* from spinach standard (Sigma-Aldrich 10865). The purity of the 5 mg/L chlorophyll *a* stock standard solution was determined spectrophotometrically as described in EPA method 445.0.

3.3.2. Phycocyanin

Phycocyanin was determined by homogenization of cells using a tissue grinder as described in Sarada et al. (1999). Samples were filtered through 47 mm, $0.7 \mu\text{m}$ pore size glass fiber filters. For each sample, a replicate was also filtered. Filters were frozen until analysis. Prior to analysis, filters were transferred to a 50 mL polycarbonate centrifuge tube and suspended in 15 mL of 50 mM phosphate buffer and broken up using a stainless steel spatula. The filter and 20 mL of buffer were homogenized for 2 min using a Teflon coated pestle. Samples were centrifuged at 5°C , 27,200 $\times g$ for 25 min using a Beckman J2-21M centrifuge. Filters were homogenized and centrifuged again using the same settings. Supernatant was collected, diluted using a 1 in 5 or 1 in 10 dilution (Sarada et al., 1999). Extracted samples were analyzed for phycocyanin concentrations fluorometrically using a TD-700 Fluorometer (Turner Designs, Inc.) equipped with a Cool White Mercury Vapor Lamp and a Phycocyanin Optical Kit (630 nm excitation and 660 nm emission filters) and calibrated using a highly purified, lyophilized powder C-phycocyanin from *Spirulina* sp. (Sigma-Aldrich P6161). Standard purity was determined spectrophotometrically using the equations of Turner. Sarada et al. (1999) reported 99% recovery of phycocyanin using the homogenization technique.

¹ The 90% buffered acetone solution was prepared by dissolving 100 mL magnesium carbonate into 900 mL acetone.

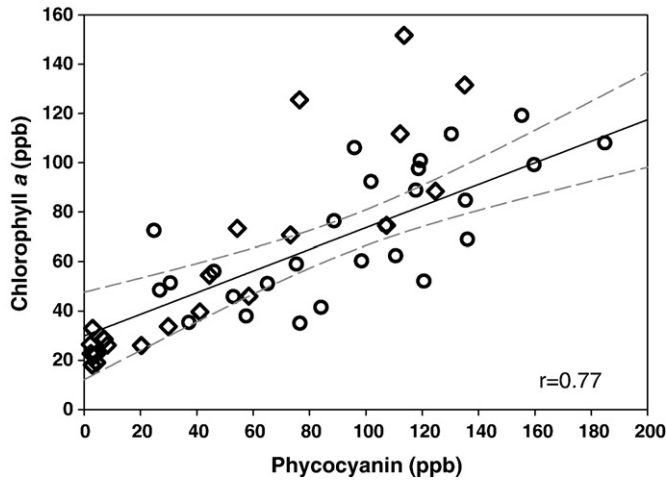


Fig. 2. Relationship between measured phytoplankton pigment concentrations, phycocyanin and chlorophyll *a*, for Morse (diamonds, *n*=23) and Geist (circles, *n*=27). Dashed 95% confidence interval for the fitted line.

3.3.3. Pigment extraction error analysis

Percent error was calculated between each sample and its replicate $\left(\frac{\bar{x}}{r}\right)$. Samples with error >30% were not used in further data analysis.

3.3.4. Phytoplankton identification and enumeration

Samples were poured into 50 mL centrifuge tubes, preserved with 0.5 mL of Lugol's solution and stored at 5 °C. Phytoplankton were identified to species and measured for biovolume. A minimum of 400 natural units were counted in each sample. Cell volumes were estimated by approximation to the nearest simple geometric solid (i.e., sphere, ovoid, or rod) (Lund et al., 1958).

3.3.5. Total suspended solids

Samples were filtered in amounts of 150–200 mL through pre-ashed, pre-weighed 47 mm, 0.7 μm pore size glass fiber filters. Samples were dried at 16 °C then placed in a desiccator. Dried and cooled samples were weighed using a Top Loading Pinnacle Series Balance (Denver Instrument Co.). TSS in mg/L was calculated by subtracting the post-weight from the pre-weight (SM2540D).

3.4. Data analysis

3.4.1. Spectral analysis

Remote sensing reflectance (R_{rs} ; sr^{-1}) was obtained using the ratio of upwelling water-leaving radiance (L_w ; $W m^{-2} sr^{-1}$) at a nadir viewing angle to the downwelling radiance (L_d ; $W m^{-2} sr^{-1}$):²

$$R_{rs} = \frac{L_w(0^+, \lambda)}{L_d(0^+, \lambda)} \quad (9)$$

The strength of the relationship between the semi-empirical algorithm estimated absorption coefficients $a_{Chl(665)}$ and $a_{PC(620)}$ and analytically measured pigment concentrations was evaluated using least-squares regression analysis, the strength of which was reported as the coefficient of determination (r^2). Confounding

parameters were investigated through a residual analysis and relative residuals (e_i) were calculated as:

$$e_i = \frac{\hat{Y}_i - Y_i}{Y_i} \quad (10)$$

Where:

- \hat{Y}_i estimated concentration of pigment *i*
- Y_i measured concentration of pigment *i*

Algorithm accuracy was reported using relative systematic error, computed as the mean of the relative residuals (MRR) and root mean square error (RMSE). Relative random error was determined using the standard deviation of the relative residuals.

4. Results and discussion

4.1. Water quality data

4.1.1. Pigments (chlorophyll *a* and phycocyanin)

A combined Morse–Geist dataset shows a large range in both phycocyanin (2–135 ppb) and chlorophyll *a* concentration (25–185 ppb). Ten sampling sites at Morse Reservoir showed phycocyanin concentrations of less than 10 ppb. A positive correlation ($r=0.77$ for a combined dataset) exists between measured chlorophyll *a* and phycocyanin pigments, where the relationship was weaker for Geist ($r=0.72$, $n=27$) than Morse ($r=0.88$, $n=23$) (Fig. 2). Morse Reservoir showed a much higher mean Phycocyanin-to-chlorophyll *a* ratio (PC: Chl*a*, 0.611), an indicator of the proportion total algal biomass that can be attributed to cyanobacteria, compared to Geist (1.35), suggesting that four times more chlorophyll *a* is present in the water column at Morse compared to phycocyanin. Overall, phycocyanin is more prevalent than chlorophyll *a* in the water column of Geist, ultimately indicative of a cyanobacteria dominated water body (Table 2).

Table 2

Summary statistics of water quality parameters for Geist and Morse Reservoirs including Secchi depth (cm), turbidity (NTU), total suspended solids (TSS), total dissolved solids (TDS), total organic carbon (TOC), chlorophyll *a* (ppb), phycocyanin (ppb), and the PC-to-Chl *a* ratio

Parameter	Mean	Median	Minimum	Maximum	σ	<i>n</i>
<i>Geist Reservoir</i>						
Secchi Depth (cm)	48	45	30	75	12	27
Turbidity (NTU)	10.3	9.8	7.0	18.0	2.1	27
TSS (mg/L)	20.4	19.4	13.2	29.2	4.2	27
TDS (g/L)	0.322	0.306	0.300	0.369	0.028	27
TOC (mg C/L)	6.2	5.9	4.4	10.3	1.2	27
Chlorophyll <i>a</i> (ppb)	71.3	64.4	34.7	118.9	26.0	27
Phycocyanin (ppb)	96.2	100.4	25.2	185.1	43.8	27
PC:Chl <i>a</i>	1.4	1.3	0.3	2.3	0.5	27
<i>Morse Reservoir</i>						
Secchi Depth (cm)	92	90	35	135	36	28
Turbidity (NTU)	6.7	4.6	2.3	30.0	6.4	28
TSS (mg/L)	15.1	8.4	4.4	54.4	15.0	28
TDS (g/L)	0.267	0.268	0.260	0.281	0.005	28
TOC (mg C/L)	5.6	5.1	4.6	7.7	0.9	28
Chlorophyll <i>a</i> (ppb)	57.2	35.6	18.0	168.6	42.9	27
Phycocyanin (ppb)	41.8	28.6	2.0	135.1	43.4	24
PC:Chl <i>a</i>	0.67	0.74	0.1	1.7	0.5	24
<i>Aggregated dataset</i>						
Secchi Depth (cm)	70	57	30	135	35	55
Turbidity (NTU)	8.5	9.1	2.3	30.0	5.2	55
TSS (mg/L)	18.1	17.2	4.4	54.4	11.7	55
TDS (g/L)	0.294	0.281	0.260	0.369	0.034	55
TOC (mg C/L)	5.9	5.8	4.4	10.3	1.1	55
Chlorophyll <i>a</i> (ppb)	64.7	57.2	18.0	168.6	36.5	54
Phycocyanin (ppb)	71.3	73.2	2.1	185.1	50.3	51
PC:Chl <i>a</i>	1.0	1.1	0.1	2.3	0.6	50

² Again, note that the skylight correction applied to total upwelling radiance (L_t) measurements in this study was similar to that of Lee et al. (1997), which suggests a value of $R_{rs}(750) > 0$ is assumed to be residual reflected sky radiance. Highly turbid waters such as these often exhibit a water-leaving radiance signal at 750 nm and therefore the signal at 900 nm, the longest wavelength not containing noise, was used to estimate L_{sky} .

4.2. Pigment extraction error analysis

4.2.1. Precision between samples and replicates

Pigment extraction precision was assessed by calculating percent error between samples and their replicates. Samples with extraction error greater than 30% were not used in further analysis. Average error was 11% and 8% for phycocyanin and chlorophyll *a*, respectively (Fig. 3). Two sampling sites, GR 238 and MR 297, were not used in further analysis due to high error (39% error for chlorophyll *a* and 66% error for phycocyanin, respectively). High error between replicate phycocyanin samples was also calculated for site MR 275 (40% error obtained from phycocyanin extraction). This site was included in further analysis because concentration of phycocyanin in the sample was very low. For extraction of both pigments, error was higher for lower concentrations.

4.2.2. Relationships between optically active constituents

Concentrations of optically active constituents in Geist do not appear to co-vary. The relationships between the pigments and turbidity and TSS at Geist yielded *r* values ranging from -0.14 – 0.39 . Weak relationships among pigment concentrations and TSS values suggest higher amounts of non-algal turbidity in the water column at Geist Reservoir (Table 2). Unlike Geist Reservoir, strong relationships ($0.75 \leq r \leq 0.93$) between phytoplankton pigments and other optically active constituents (OACs), (*i.e.*, turbidity and TSS) were observed in Morse Reservoir. High correlations between pigment concentration and TSS measurements at Morse suggest that, on the day sampled, turbidity is mostly a function of phytoplankton abundance in the water column.

4.2.3. Algorithm application

Reflectance spectra from Geist and Morse Reservoirs contained the classic features identified for turbid, productive waters (Fig. 4a and b). Sources of and shifts in the position and magnitude of the features found in the spectra based on water chemistry have been discussed at length in previously published work (*i.e.*, Gordon and Morel, 1983; Dekker et al., 1991; Gitelson et al., 1986; Schalles and Yacobi, 2000).

4.2.4. Chlorophyll *a*

Application of the Simis et al. (2005) algorithm to Geist Reservoir data for retrieval of chlorophyll *a* from $a_{\text{chl}}(665)$ yielded a relatively weak relationship ($r^2=0.40$, $p<0.001$, $n=27$) between measured and

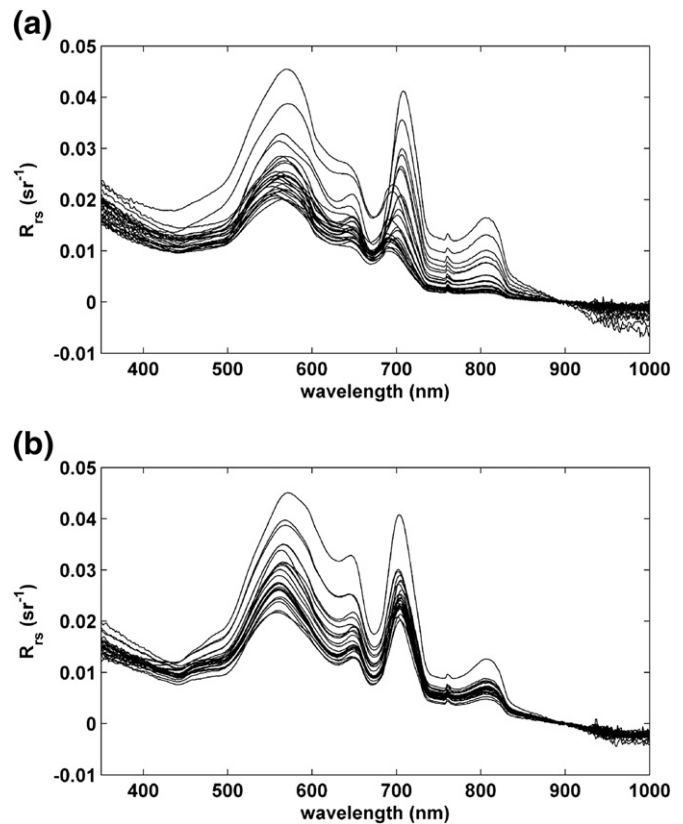


Fig. 4. a and b: Remote sensing reflectance, R_{rs} (sr^{-1}) measured at (a) 27 sites on Geist Reservoir and (b) 28 sites on Morse Reservoir.

estimated chlorophyll (Table 3, Fig. 5a and b). Estimation of chlorophyll concentration by employing $a_{\text{chl}}^*(665)$, as reported by Simis et al. (2006) for various lakes and reservoirs in Spain and The Netherlands, yielded a RMSE of 25.39 and MRR of 0.305 ($\sigma=0.407$). Relative residual values decreased with increasing chlorophyll *a* concentration ($r=-0.73$), with two sampling sites (GR 247 and 248) exhibiting low overall chlorophyll *a*, and low Chl:TSS ratios (34.71 ppb, 0.0017 and 41.16 ppb, 0.0066, respectively) yielding the highest relative residuals values of 1.41 and 1.42. Thus, this deviation is caused by a low proportion of the total suspended material at these locations attributed to chlorophyll *a*. The signal is instead dominated by non-algal material. For both sites, the model overestimated chlorophyll *a* concentration.

The algorithm proved more successful for retrieval of chlorophyll *a* from $a_{\text{chl}}(665)$ for Morse Reservoir data, yielding a strong relationship ($r^2=0.77$, $p<0.001$, $n=26$) between estimated and analytically measured chlorophyll *a* concentrations (Table 3, Fig. 5a and b). Morse Reservoir estimated chlorophyll *a* yielded a RMSE of 23.26 ppb and MRR of 0.059 ($\sigma=0.309$). Again, the maximum relative residual value (0.973; site 294) was obtained where Chl:TSS was low (0.002), suggesting high influence of non-algal material (Table 3, Fig. 5b). The same trend holds for sites with moderately high relative residual values (0.42; site 295) where relatively low Chl:TSS exists (0.0025). For these sites, as for Geist, the Simis et al. (2005) algorithm underestimated chlorophyll *a* concentration. Conversely, sites exhibiting high Chl:TSS (0.0054–0.0060) ratios were typically underestimated by the Simis et al. algorithm, producing negative relative residuals (-0.19 to -0.34).

When applied to an aggregated dataset (combining the samples from both reservoirs), an r^2 value of 0.69 ($p<0.001$, $n=53$) was obtained from the linear least-squares regression of algorithm estimated to analytically measured chlorophyll *a* (Table 3, Fig. 5a and b). The

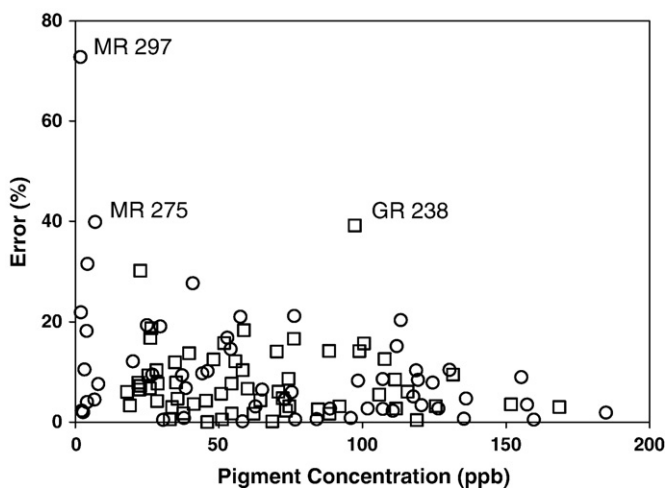


Fig. 3. Relationship between fluorometrically measured chlorophyll *a* (squares) and phycocyanin (circles) and error (%) between samples and their replicates. Mean error is 8% ($n=60$) and 11% ($n=57$), respectively.

Table 3

Performance summary of the Simis et al. (2005) algorithm for estimation of chlorophyll *a* concentration for Geist ($n=27$) and Morse ($n=26$) Reservoirs and for a combined dataset ($n=53$) including the linear least-squares fit (r^2), slope and intercept between [Chl a] measured and [Chl a] estimated with their corresponding standard error of estimation (STE), the root mean square error (RMSE), and the mean and standard deviation of relative residuals

	Reservoir	Intercept (STE)	Slope (STE)	Mean/ standard deviation of relative residual	r^2 (p-value)	min/max relative residual	RMSE (ppb)	n
Simis et al. (2005) semi-empirical algorithm	Geist	52.65 (8.57)	0.47 (0.11)	0.305 (0.407)	0.40 ($p<0.001$)	-0.20 (1.42)	25.39	27
	Morse	4.18 (5.19)	0.74 (0.07)	0.059 (0.309)	0.77 ($p<0.0001$)	-0.34 (0.97)	23.26	26
	Combined	15.69 (7.29)	0.90 (0.09)	0.184 (0.380)	0.69 ($p<0.0001$)	-0.20 (1.42)	23.89	53

aggregated dataset yielded a RMSE and 23.89 ppb and MRR of 0.184 ($\sigma=0.380$).

4.2.5. Phycocyanin

Application of the Simis et al. (2005) algorithm for retrieval of phycocyanin from $a_{PC}(620)$ for Geist and Morse Reservoir data yielded r^2 values of 0.75 ($p<0.0001$, $n=25$) and 0.91 ($p<0.0001$, $n=23$), respectively (Table 4, Fig. 6a and b). Estimated phycocyanin concentration was obtained using the phycocyanin specific absorption coefficient at 620 nm, $a_{PC}^*(620)$, reported by Simis et al. (2006) as the average $a_{PC}^*(620)$ value for various lakes and reservoirs in Spain and The Netherlands. Results reported here were comparable to those obtained by Simis et al. (2005), where the relationship between measured and estimated PC concentrations for a combined dataset (including samples from Lakes IJsselmeer and Loosdrecht, The Netherlands) yielded r^2 values of 0.94 (where slope and intercept values of 0.99 and 0.53, respectively resulted). However, the aforementioned relationship was obtained using site specific $a_{PC}^*(620)$ values. When employing a fixed specific absorption coefficient ($a_{PC}^*(620)=0.0095 \text{ m}^2$), Simis et al. (2005) reported a weaker relationship ($r^2=0.77$ with slope and intercept values of 0.59 and 29.03 respectively).

Comparison of estimated to measured phycocyanin concentration for Geist Reservoir yielded a RMSE of 22.5 ppb and MRR of 0.074 ($\sigma=0.317$; Table 4, Fig. 6b). A strong negative correlation ($r=-0.77$) resulted between measured phycocyanin and relative residual values, where the sampling site with the largest relative residual (GR 262) also proved to have the lowest analytically measured phycocyanin concentration (25.20 ppb; Fig. 6b). The model overestimated phycocyanin at this site by approximately 26 ppb (Fig. 5b). The largest negative relative residual values (-0.28 and -0.32) were found at sites GR 236 and GR 241, where the highest phycocyanin concentrations were measured (155.56 and 159.93 ppb, respectively). A strong correlation ($r=0.81$) also resulted between the PC:TSS ratio and phycocyanin relative residual values, where $a_{PC}(620)$ and thus phycocyanin concentration was overestimated for sites with high concentrations of suspended material not dominated by phycocyanin and underestimated for sites with TSS regimes with high cyanobacterial abundance.

The algorithm appears to have difficulty in distinguishing between sites with concentrations measuring 110–160 ppb, ultimately underestimating phycocyanin concentration producing relative residual values of -0.08 to -0.32. Several possible explanations exist as the cause of such an underestimation of PC at high concentrations. A non-linear relationship between PC concentration and absorption at 620 nm where, at higher concentrations, the pigment does not as efficiently absorb energy, may exist. Specifically, pigment packaging is known to reduce absorption per PC concentration unit, whereby an underestimation of total concentration would result (Simis et al., 2007). Photoadaptation likewise remains unaccounted for, where self-shading processes, the repositioning of pigment position within a cell to appropriately adapt to the current light field, could present a non-

linear relationship between extracted pigment concentration and absorption. *In-vivo* measurements of $a_{PC}(620)$ could be helpful in investigating pigment packaging effects.

An additional identified source for underestimation of PC at high concentrations is born from the assumption that the absorption by phytoplankton pigments at 709 nm is negligible, thus absorption at

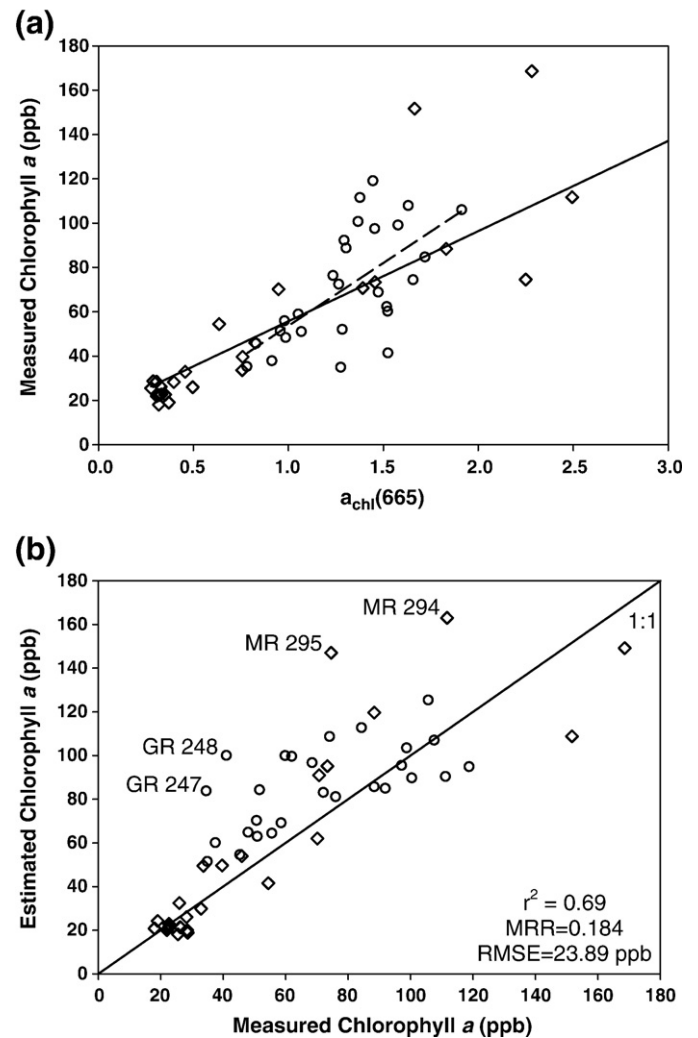


Fig. 5. a and b: algorithm-derived absorption coefficients for chlorophyll *a*, $a_{chl}(665)$, versus analytically measured chlorophyll *a* concentrations for Geist (circles; $r^2=0.40$, dashed line; $n=27$) and Morse (diamonds; $r^2=0.74$, solid line; $n=26$), and (b) analytically measured chlorophyll *a* concentrations versus estimated concentrations using $a_{chl}(665)$ for Geist (circles; MRR=0.305; RMSE=25.39 ppb) and Morse (squares; MRR=0.059; RMSE=23.26 ppb). Labels indicate sites with the highest relative residual values.

Table 4
Performance summary for the Simis et al. (2005) algorithm for estimation of phycocyanin concentration for Geist ($n=25$) and Morse Reservoirs ($n=23$) and for a combined dataset ($n=48$) including the linear least-squares fit (r^2), slope and intercept between [PC] Measured and [PC] Estimated with their corresponding standard errors of estimation (STE), the root mean square error (RMSE), and the mean and standard deviation of relative residuals

	Reservoir	Intercept (STE)	Slope (STE)	Mean/standard deviation of relative residual	r^2 (p-value)	min/max relative residual	RMSE (ppb)	n
Simis et al. (2005) semi-empirical algorithm	Geist	34.76 (7.03)	0.58 (0.07)	0.074 0.317	0.75 ($p<0.0001$)	-0.32 1.03	22.15	25
	Morse	8.81 (4.24)	1.00 (0.07)	0.981 1.923	0.91 ($p<0.0001$)	1.10 8.48	17.40	23
	Combined	16.59 (4.13)	0.80 (0.05)	0.51 1.41	0.85 ($p<0.0001$)	-0.32 8.48	19.54	48

this location is attributed only to pure water. The absorption coefficient of a pigment will be underestimated if that pigment is absorbing energy at 709 nm. The likelihood of a pigment absorbing at longer wavelengths would increase as the concentration of that pigment in the water column increases. An underestimation of $a_{PC}(620)$ would cause a subsequent underestimation in retrieved pigment concentration that will increase with measured concentration. This assumption could be the cause of the consistent underestimation

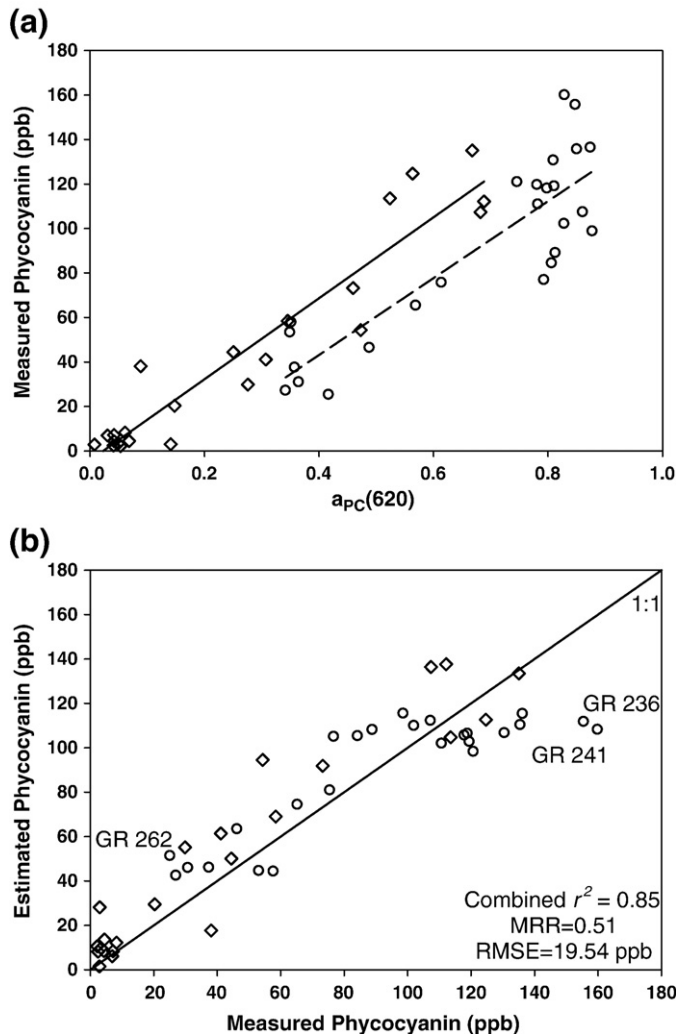


Fig. 6. a and b: Simis et al. (2005) algorithm-derived absorption coefficients for phycocyanin at 620 nm ($a_{PC}(620)$) versus analytically measured phycocyanin concentrations for Geist (circles; $r^2=0.75$, dashed line; $n=25$) and Morse (squares; $r^2=0.91$, solid line; $n=23$), and (b) analytically measured phycocyanin concentrations versus estimated concentrations using $a_{PC}^*(620)$ for Geist (circles; $MRR=0.074$; $RMSE=22.15$ ppb) and Morse (diamonds; $MRR=0.981$; $RMSE=17.40$ ppb).

of phycocyanin concentration for sampling sites with measured phycocyanin of greater than 120 ppb.

The algorithm retrieval of phycocyanin concentration from $a_{PC}(620)$ resulted in a strong relationship ($r^2=0.91$, $p<0.0001$, $n=23$) with measured phycocyanin concentrations for Morse Reservoir, producing a RMSE of 17.40 ppb and MRR of 0.981 ($\sigma=1.923$; Table 4, Fig. 6). A single outlier (GR 271) exists in the dataset, where a relative residual value of 8.48 resulted. The highest of the remaining relative residuals are associated with sampling sites with phycocyanin concentrations less than 10 ppb, where the algorithm is reported to always produce and overestimation. Overestimation at these sites is likely attributable to underestimation or exclusion of absorption by other pigments at 620 nm, including error in estimation of ϵ . Further pigment analysis performed by Simis et al. (2006) suggested the aforementioned overestimations of PC could be attributed to increased absorption by accessory chlorophyll pigments in addition to chlorophyll *a*. Chlorophyll *b*, for which 600 nm is the location of a second absorption feature and chlorophyll *c*, with absorption maxima at 580 and 630 nm, are known to present in green algae and diatoms, respectively, both highly abundant in Morse Reservoir. Unfortunately, these pigments were not analyzed as a part of this study.

Further error is likewise introduced through the application of an average $a_{PC}^*(620)$ to low concentration areas for retrieval of PC estimation, where the specific absorption coefficient would be higher than for high concentration waters.

When applied to a combined dataset, an r^2 value of 0.85 ($p<0.0001$, $n=48$) was obtained from the linear least-squares regression of estimated to analytically measured phycocyanin (Table 4, Fig. 6a and b). The combined dataset yielded a RMSE of 19.54 and MRR of 0.51 ($\sigma=1.41$).

4.3. Evaluation of phycocyanin pigment concentration as a measure of blue-green algal abundance

To ensure that the remote sensing of optically active pigments, phycocyanin and chlorophyll *a*, is an accurate method for estimating *in-vitro* phytoplankton pigment concentrations, the relationship between spectral response and extracted phycocyanin and chlorophyll *a* was determined. The relationship between *in-vitro* phytoplankton pigment concentration and measures of blue-green algal biomass and biovolume ultimately determines the effectiveness of remote sensing of phytoplankton pigments as a proxy for blue-green algal abundance. In the case that cyanobacterial biovolume is strongly correlated with chlorophyll *a* concentration then chlorophyll *a*, a proxy widely used to estimate phytoplankton abundance, can be employed to determine biomass, while the $a_{PC}(620)$ feature becomes an indication of cyanobacterial presence or absence. A subset of 25 samples was randomly selected from an aggregated dataset and analyzed for phytoplankton identification, enumeration, and biovolume, a density measure of blue-green cell biomass. A strong relationship ($r^2=0.80$, $p<0.0001$; Fig. 7a) between measured phycocyanin concentrations and biovolume measurements was observed. Measures of blue-green algal biovolume can

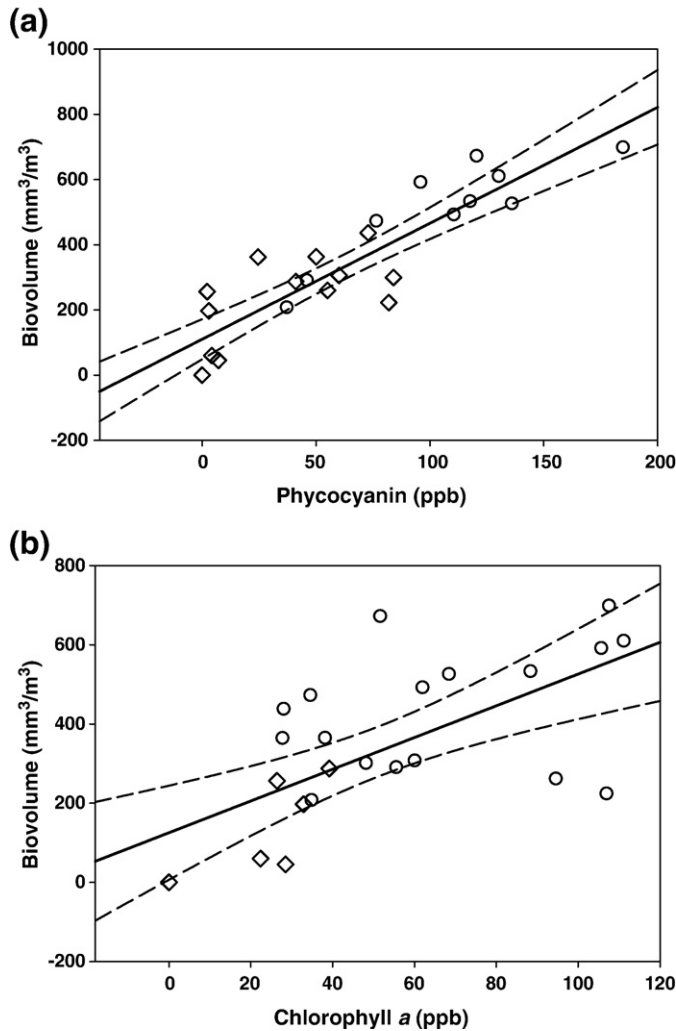


Fig. 7. Relationship between (a) phycoerythrin ($r^2=0.80$, $p<0.0001$, $n=25$) and (b) chlorophyll *a* ($r^2=0.43$, $p<0.001$, $n=25$) concentrations and measures of blue-green algal biovolume. Dashed lines delineate the 95% confidence interval for the fitted line.

be determined from phycoerythrin concentration using the equation obtained from the linear least-squares regression of measured phycoerythrin concentration to blue-green biovolume from the 25 sample subset (Eq. (13)):

$$\text{Blue-green Biovolume (mm}^3/\text{m}^3) = 110.1 + (3.56 \times [\text{PC}] (\text{ppb})) \quad (13)$$

$$\text{Blue-green Biovolume (mm}^3/\text{m}^3) = 125.2 + (4.01 \times [\text{Chl}] (\text{ppb})) \quad (14)$$

Using the relationship between cyanobacteria biovolume and phycoerythrin concentration from the linear least-squares regression yielded a mean relative residual of 0.11 (median = -0.003, $\sigma=0.55$) for estimated phycoerythrin concentration. A comparatively weaker relationship was found between chlorophyll *a* concentration and cyanobacterial biomass ($r^2=0.43$; Fig. 7b), whereby employing the linear least-squares relationship between chlorophyll *a* and blue-green algal biovolume (Eq. (14)) yielded a mean relative residual of 0.33 (median = -0.06, $\sigma=1.12$). Ultimately, phycoerythrin concentration proves to be the most accurate proxy for cyanobacterial abundance, where for a large range in biomass, predictability is strong.

Algal biovolume was measured because variation in the size and shape of algal cells cannot be accounted for when performing phytoplankton counts, but can when measuring algal biovolume. Sampling sites with high algal counts could have low algal biovolume

if the taxa present are small in size. For example, a potential explanation for Morse Reservoir sampling site 274 being an outlier could be that the sample is dominated by small taxa, accounting for 77% of the natural units but only 21% of the biovolume. The disparity was caused by the prevalence of small blue-green taxa, such as *Merismopedia minima* and *Pseudanabaena limnetica*, which contribute little to overall biovolume and phycoerythrin concentrations but can dominate counts. The strong relationship observed between *in-vitro* pigment concentration and blue-green algal biovolume suggests measurements of pigment concentration could be an accurate measure of blue-green algal abundance.

4.4. Accuracy assessment of field-based remote sensing technique for phycoerythrin estimation

The data presented suggests that multi and hyperspectral remote sensing, coupled with the Simis et al. (2005) semi-empirical algorithm for estimation of phycoerythrin pigment concentration in inland, productive water has potential to be an effective method for rapid cyanobacteria bloom assessment. The successful extension of this method, however, would require the measurement and detailed analysis of the IOPs of these and similar systems under varying conditions before application. The inclusion of two, optically distinct systems in this study gives an indication of the effect of differing water chemistry on the algorithm performance and provides insight into avenues for further tuning and investigation. Though a relatively strong relationship resulted from the linear least-squares regression of the algorithm estimated phycoerythrin absorption and analytically measured pigment concentrations ($r^2=0.85$, $p=0.0001$; MRR=0.51, RMSE=19.54 ppb), several potential sources of error exist in estimation including: error in the estimation of pigment specific absorption coefficients, change in pigment absorption efficiency, the presence of non-algal particles and thus the estimate of b_b , and error in prediction for non-cyanobacteria dominated waters.

4.5. Error associated with algorithm application

The specific absorption coefficients used for retrieval of pigment concentrations in this study were the average of those measured by Simis et al. (2005 and 2006) at various lakes and reservoirs in Spain and The Netherlands. Though application of the fixed specific absorption coefficient to Indianapolis reservoir data was generally successful, some of the high phycoerythrin estimation error produced could be the result of this extension (from European data) and simplification. According to Simis et al. (2005), high variability exists in phycoerythrin specific absorption coefficients, as was seen in data obtained from Lakes Loosdrecht and IJsselmeer (The Netherlands) and an inverse relationship between the PC:Chl *a* ratio and the specific absorption coefficient for cyanobacteria at 620 nm was identified. Thus, for low concentrations of phycoerythrin, low $a_{\text{PC}}(620)$, $a_{\text{PC}}^*(620)$ should be higher compared to that of cyanobacteria dominated waters and application of a fixed to $a_{\text{PC}}^*(620)$ sites exhibiting low phycoerythrin consistently would yield an overestimation of pigment concentration, as was seen in the Simis et al., 2005 and 2006 application. This may have produced error in phycoerythrin estimation in Morse Reservoir data, where phycoerythrin concentrations measuring 2–10 ppb were estimated to have 19–33 ppb phycoerythrin and relative residuals ranging from 2.35 to 8.48. As previously noted, the contribution of absorption by pigments unaccounted for in this study (specifically chlorophylls *b* and *c*) could also be producing elevated $a_{\text{PC}}(620)$ values and subsequent overestimations of phycoerythrin concentration.

Pigment absorption efficiency is also suggested to be a function of season, environmental conditions, nutrient and light availability, phytoplankton composition and species competition (Tandeau De Marsac, 1977; Metsamaa et al., 2006). Only a single season, thus one temperature and irradiance regime, has been tested in this study, ultimately limiting its value since the relationship between phycoerythrin concentration and

cyanobacterial abundance has been known to change as a result of these conditions. Different strains of cyanobacteria also exhibit different absorption efficiencies per mass unit (Ahn et al., 1992; Metsamaa et al., 2006). This identified source of error could be one potential explanation for the underestimation of phycocyanin concentrations for Geist Reservoir sites, where measured pigment concentrations were greater than 100 ppb. It is possible that, at high concentrations, pigments no longer absorb energy proportional to concentration; rather absorption efficiency of the cyanobacterial cell stabilizes, causing a deviation from the linear relationship between the estimated concentration using the absorption coefficient and measured phycocyanin concentrations above 100 ppb. This however, cannot be confirmed in this study since total PC concentration in the water sample was measured and intracellular PC unknown.

Another simplification employed by the Simis et al. (2005) algorithm is introduced by the assumption that absorption by phytoplankton pigments at 709 nm is insignificant or absent (absorption here is attributed to pure water only) and absorption by non-algal material is not considered. The first simplification is assumed to cause a potential underestimation of pigment concentration. Absorption at 709 nm by phytoplankton pigments will increase as concentration increases, resulting in a miscalculation of the absorption coefficient. To adjust for the simplification, Simis et al. (2005) proposed the use of a correction factors (γ and δ) obtained by relating laboratory-measured to algorithm-derived phycocyanin absorption coefficients. The correction factors calculated and employed by Simis et al. (2005) were applied for this study. Application of this correction was successful for Morse Reservoir, where concentration of non-algal material was low. The correction proved less successful however, for Geist Reservoir, where concentrations of non-algal material were high.

Backscattering, calculated from $R_{rs}(778)$, is also assumed invariant between the red and NIR bands employed, suggesting that the influence of other optically active constituents on remote sensing reflectance shows little to no variation spectrally. This assumption is supported by previous investigations in similarly complex, case II waters (i.e. Gons, 1999), however the Indianapolis reservoirs are small and serve large watersheds, terrestrial influence is particularly high and the input material is compositionally complex (particle size, shape, and refractive indices). Thus, b_b shape could therefore be spectrally dependent. A bias toward overestimation of PC and Chl concentrations exist when the pigment:TSS ratios decrease, suggesting that backscattering is not invariant between the bands used in the ratio. This error and the associated relationship to low pigment:TSS ratios is likely induced by the presence of non-algal material.

Ultimately the semi-empirical algorithm introduced by Simis et al. (2005) is suggested to function best in cyanobacteria dominated

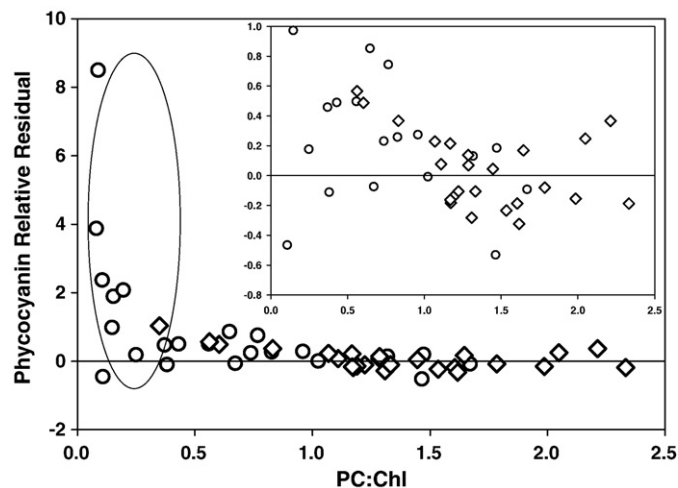


Fig. 8. Measures of PC:Chl for Indianapolis reservoir sites and associated relative residuals of estimated phycocyanin concentration. Inset graph excludes squared values.

systems. This assumption was supported by this study. As the ratio of phycocyanin-to-chlorophyll *a* decreases, error in the estimation of phycocyanin concentration increases. Simis et al. (2005) specifically identifies an acute increase in estimation error for waters with PC:Chl of less than 0.4. This threshold was observed in Indianapolis reservoir data. For sites with $PC:Chl \geq 0.5$, relative residuals remained within -0.01 and 0.65 (Fig. 8). A previously mentioned potential source of error in PC estimation for sites with low PC concentration was focused on the employed chlorophyll *a* correction ($\epsilon=0.24$) scheme proposed by Simis et al. (2005) for removing absorption at 620 nm attributed to chlorophyll *a* pigment is for cyanobacteria dominated waters. Under such conditions, the proportion of total absorption at 620 nm attributed to chlorophyll *a* is estimated as 24% of $a_{Chl}(665)$. For chlorophyll dominated waters, this ϵ factor underestimates absorption by chlorophyll *a* at 620 nm, causing an over estimation of $a_{Chl}(620)$ and ultimately PC pigment concentration. A more appropriate estimate of $a_{Chl}(620)$ for chlorophyll *a* dominated water ($\epsilon=0.3$; Bidigare et al., 1990) should therefore be applied. Employing the correction to Morse Reservoir sites where $0.09 \leq PC:Chl \leq 0.197$, reduced relative residuals by 0.54 to 2.19.

4.6. Error related to data collection

Errors introduced by data collection rather than algorithm application also exist. To minimize effects of atmospheric interference, data were collected under cloudless, dry sky conditions where intensity of solar irradiance was constant. A total of 15 spectra were averaged for each site, optimizing the signal-to-noise ratio and, thus error induced by *in-situ* measurement. The optical fiber was positioned at nadir on a mount extending away from the boat to reduce the influence of reflectance off of the vessel on collected spectra. Though the water was placid, the potential for error due to skylight reflection exists. A viewing geometry where the optical fiber is positioned at a 45° angle from nadir to avoid skylight reflection has been suggested and should be employed in future campaigns (Mobley, 1999). A skylight reflection correction was not applied in this study, however empirical relationships employed likely reduce the error resulting from skylight reflection since this error is likely to affect reflectance along the spectral range of interest similarly.

4.7. Error introduced in analytical analysis

Error in the estimated values obtained using the Simis semi-empirical algorithm could also have arisen from the analytical method used for pigment extraction. Though several methods for phycocyanin extraction have been tested, adequate validation for these methods has not yet been provided, thus no method is widely accepted. Simis et al. (2005) suggested that low extraction efficiency would result in an overestimation of the phycocyanin specific absorption coefficient and a corresponding underestimation of phycocyanin concentration. It is possible that, because the average specific absorption coefficient obtained from Lakes Loosdrecht and IJsselmer data was high, higher pigment extraction efficiency was obtained in this study.

5. Conclusions

Overall the Simis et al. (2005) semi-empirical algorithm for retrieval of phycocyanin pigment concentration and estimation of blue-green algal abundance showed promising results suggesting that, after further investigation and subsequent reduction in the aforementioned sources of error, the algorithm could be robust and may be transferable to other turbid, productive systems. It is important to note however, that the data used here for algorithm validation was collected on only two summer days (when cyanobacterial abundance is known to be high) at two compositionally and optically unique reservoirs. Therefore, this study did not capture the seasonal variability necessary for a more complete validation procedure. It instead serves as the initial step for investigating the utility of a semi-empirical remote

sensing method as a rapid assessment tool for the spatial distribution and relative concentration of blue-green algae. This study does suggest that remote sensing shows promising potential for providing an efficient method for tracking blue-green algal occurrence over time and informing management strategies, indicating areas for treatment and mitigation. Likewise, the effectiveness of employed management strategies for controlling algal abundance can be efficiently measured using remote sensing methods.

While the ultimate goal in most water quality remote sensing investigations is focused on the development and validation of algorithms for air and space-borne applications, considering the logistical difficulties of airborne image collection and both the coarse spatial and spectral resolution of satellite imagery, for some managers, field-based techniques like the approach used in this study, are optimal for lake assessment. Managers of drinking and recreational waters are desperate for a rapid assessment method that field-based remote sensing has the potential to provide, since water collection and testing is a laborious process. Though the use of remote sensing could never replace water sample analysis, it can however, inform managers of the most at risk locations, thus where and when to collect water. This information is invaluable, considering the heterogeneous and ephemeral nature of cyanobacterial blooms.

With the hope of continued improvement in both the spatial and spectral resolution of space-borne systems, further tuning and validation on the Simis et al. (2005) algorithm should be explored using field spectroscopy and the measurement of IOPs. Extension of the improved algorithm to imagery collected using airborne systems, such as Airborne Imaging Spectroradiometer for Applications (AISA) with 1 m spatial resolution and 20 spectral bands (including one centered at 620 nm) will facilitate high spatial resolution mapping of the relative concentration and distribution of cyanobacteria in inland, productive water. By indicating the relative abundance of blue-green algae, this remote sensing technique can be employed to inform sampling campaigns for monitoring toxin production potential statewide. Coupled with physical and chemical data from the reservoirs, remote sensing of cyanobacteria can aid in understanding bloom formation and can facilitate predicting bloom occurrence and subsequent toxin production.

Acknowledgements

Funding for this research was provided by the Indiana Department of Natural Resources Lake and River Enhancement Program and by Veolia Water Indianapolis, LLC. The authors thank the students, staff and faculty in the Department of Earth Sciences at IUPUI for participating in the field sampling campaign. We thank five anonymous reviewers for their careful consideration and critique of the analyses presented here. We also thank Rebecca Sengpiel and Veolia Water White River Laboratories for assisting in analytical analyses.

References

Ahn, Y., Bricaud, A., & Morel, A. (1992). Light backscattering efficiency and related properties of some phytoplankters. *Deep-Sea Research*, 39(11/12), 1835–1855.

Astoreca, R., Ruddick, K., Rousseau, V., Van Mol, B., Parent, J., & Lancelot, C. (2006). Variability of the inherent and apparent optical properties in a highly turbid coastal area: impact on the calibration of remote sensing algorithms. *EARSEL eProceedings*.

Backer, L. C. (2002). Cyanobacterial harmful algal blooms: developing a public health response. *Lake and Reservoir Management*, 18(1), 20–31.

Bidigare, R. R., Ondrusek, M. E., Morrow, J. H., & Keifer, D. A. (1990). *In vivo* absorption properties of algal pigments. *SPIE Ocean Optics X*, 1302, 290–302.

Buiteveld, H., Hakvoort, J., & Donze, M. (1994). The optical properties of pure water. *Ocean Optics XII Proc Soc Photoopt Eng* 2258 (pp. 174–183).

Dekker, A. (1993). *Detection of the optical water quality parameters for eutrophic waters by high resolution remote sensing*. Amsterdam: Free University Ph.D.

Dekker, A., Malthus, T., & Seyhan, E. (1991). Quantitative modeling of inland water-quality for high-resolution MSS-systems. *IEEE Transactions on Geoscience and Remote Sensing*, 29(1), 89–95.

Gitelson, A., Garbuzov, G., Szilagyi, F., Mittenzwey, K. -H., Karnieli, A., & Kaiser, A. (1993). Quantitative remote sensing methods for real-time monitoring of inland water quality. *International Journal of Remote Sensing*, 14, 1269–1295.

Gitelson, A., Nikanorov, A., Sabo, G., & Szilagyi, F. (1986). Etude de la qualite des eaux de surface par teledetection. *IAHS Publications*, 157, 111–121.

Gitelson, A., Schalles, J., Rundquist, D., Schiebe, F., & Yacobi, Y. (1999). Comparative reflectance properties of algal cultures with manipulated densities. *Journal of Applied Phycology*, 11, 345–354.

Gons, H. (1999). Optical teledetection of chlorophyll *a* in turbid inland waters. *Environmental Science Technology*, 33, 1127–1132.

Gordon, H., Brown, O., Evans, R., Brown, J., Smith, R., Baker, K., et al. (1988). A semi-analytical radiance model of ocean color. *Journal of Geophysical Research*, 93, 10909–10924.

Gordon, H., Brown, O., & Jacobs, M. (1975). Computed relationships between the inherent and apparent optical properties of a flat homogeneous ocean. *Journal of Applied Optics*, 14, 417–427.

Gordon, H., & Morel, A. (1983). *Remote assessment of ocean color for interpretation of satellite visible imagery: A review*. New York and Berlin: Springer-Verlag.

Indiana Department of Environmental Management (2002). *Indiana integrated water quality monitoring and assessment report*. IDEM/34/02/004/2002.

Indiana Department of Environmental Management (2004). *Indiana integrated water quality monitoring and assessment report*. <http://www.in.gov/idem/water/planbr/wqs/quality.html>

Indiana Department of Environmental Management (2006). *Indiana integrated water quality monitoring and assessment report*. <http://www.in.gov/idem/water/planbr/wqs/quality.html>

Jupp, D., Kirk, J., & Harris, G. (1994). Detection, identification, and mapping of cyanobacteria – Using remote sensing to measure the optical quality of turbid inland waters. *Australian Journal of Marine and Freshwater Research*, 45, 801–828.

Kirk, J. T. O. (1994). *Light and Photosynthesis in Aquatic Ecosystems*, 2nd ed. Cambridge, UK: Cambridge University Press 509 pp.

Lee, Z. P., Carder, K. L., Steward, R. G., Peacock, T. G., Davis, C. O., & Mueller, J. L. (1997). Remote-sensing reflectance and inherent optical properties of oceanic waters derived from above water measurements. In S. G. Ackleson & R. Frouin (Eds.), *Ocean Optics XIII Proc. SPIE*, vol. 2963 (pp. 160–166).

Lee, Z. P., Du, K., Arnone, R., Liew, S. C., & Penta, B. (2005). Penetration of solar radiation in the upper ocean – A numerical model for oceanic and coastal waters. *Journal of Geophysical Research*, 110, C09019. doi:10.1029/2004JC002780.

Lund, J., Kipling, C., & LeCren, E. (1958). The inverted microscope method of estimating algal numbers and the statistical basis of estimations by counting. *Hydrobiologia*, 11, 143–170.

Maritorena, S., & Siegel, D. A. (2005). Consistent merging of satellite ocean color data sets using bio-optical model. *Remote Sensing of Environment*, 94, 429–440.

Metsamaa, L., Kutser, T., & Strombeck, N. (2006). Recognising cyanobacterial blooms based on their optical signature. *Boreal Environmental Research*, 11, 493–506.

Mittenzwey, K., & Gitelson, A. (1988). *In-situ* monitoring of water quality on the basis of spectral reflectance. *Internationale Revue der gesamten Hydrobiologie*, 73, 61–72.

Mittenzwey, K., Ullrich, S., Gitelson, A., & Kondratiev, K. (1992). Determination of chlorophyll *a* of inland waters on the basis of spectral reflectance. *American Society of Limnology and Oceanography*, 37, 147–149.

Mobley, C. D. (1999). Estimation of the remote-sensing reflectance from above-surface measurements. *Applied Optics*, 38, 7442–7455.

Morel, A. (2001). Bio-optical Models. In J. H. Steele, K. K. Turekian & S.A. Thorpe (Eds.), *Encyclopedia of Ocean Sciences* (pp. 317–326). New York: Academic Press.

Morel, A., & Gentili, B. (1991). Diffuse reflectance of oceanic waters – Its dependence on sun angle as influenced by the molecular scattering contribution. *Applied Optics*, 30, 4427–4438.

Morel, A., & Gordon, H. (1980). Report of the working group on water color. *Boundary-Layer Meteorology*, 18, 343–355.

Morel, A., & Prieur, L. (1977). Analysis of variation in ocean color. *Limnology and Oceanography*, 37, 147–149.

Pitois, S., Jackson, M., & Wood, B. (2000). Problems associated with the presence of cyanobacteria in recreational and drinking waters. *International Journal of Environmental Health Research*, 10, 203–218.

Pope, R. M., & Fry, E. S. (1997). Absorption spectrum (380–700 nm) of pure water. *Applied Optics*, 36, 8710–8723.

Preisendorfer, R. W. (1976). *Hydrologic Optics*, V. 5: Properties (NTIS PB-259 797/9ST). Springfield: NTIS.

Sarada, R., Pillai, M., & Ravishankar, G. (1999). Phycocyanin from *Spirulina* sp: Influence of processing of biomass on phycocyanin yield, analysis of efficacy of extraction methods and stability studies on phycocyanin. *Process Biochemistry*, 34, 795–801.

Schalles, J., & Yacobi, Y. (2000). Remote detection and seasonal patterns of phycocyanin, carotenoid and chlorophyll pigments in eutrophic waters. *Archive Hydrobiological Special Issues Advance Limnological*, 55, 153–168.

Simis, S., Peters, S., & Gons, H. (2005). Remote sensing of the cyanobacterial pigment phycocyanin in turbid inland water. *American Society of Limnology and Oceanography*, 50(11), 237–245.

Simis, G. H., Ruiz-Verdú, A., Dominguez-Gómez, J. A., Peña-Martinez, R., Peters, S. W., & Gons, H. J. (2006). Influence of phytoplankton on remote sensing of cyanobacterial biomass. *Remote Sensing of Environment*, 106, 414–427.

Simis, S., Ruiz-Verdú, A., Dominguez-Gómez, J., Peña-Martinez, R., Peters, S., & Gons, H. (2007). Influence of phytoplankton pigment composition on remote sensing cyanobacterial biomass. *Remote Sensing of Environment*, 106, 414–427.

Tandau De Marsac, N. (1977). Occurrence and nature of chromatic adaptation in cyanobacteria. *Journal of Bacteriology*, 130(1), 82–91.

Tedesco, L., Atekwana, E., Filippelli, G., Licht, K., Shrake, L., Hall, B., et al. (2003). Water quality and nutrient cycling in three Indiana watersheds and their reservoirs: Eagle Creek/Eagle Creek Reservoir, Fall Creek/Geist Reservoir and Cicero Creek/Morse Reservoir. *Central Indiana Water Resources Partnership. CEES Publication 2003-01, IUPUI, Indianapolis, IN* 163 pp.

Tedesco, L., Pascual, D., Shrake, L., Casey, L., Hall, B., Vidon, P., Hernly, F., Barr, R., Ulmer, J., & Pershing, D. (2005). Eagle Creek Watershed Management Plan: An Integrated Approach to Improved Water Quality. *Eagle Creek Watershed Alliance, CEES Publication 2005-07, IUPUI, Indianapolis, IN* 182 pp.